Journal of Photochemistry and Photobiology A: Chemistry 306 (2015) 31–40

Contents lists available at ScienceDirect

Journal of Photochemistry and Photobiology A: Chemistry

journal homepage: www.elsevier.com/locate/jphotochem

Axially paraben substituted silicon(IV) phthalocyanines towards dental pathogen *Streptococcus mutans*: Synthesis, photophysical, photochemical and *in vitro* properties

Gökçe Canan Taşkın [a], Mahmut Durmuş [a], Fatma Yüksel [a], Vanya Mantareva [b,**], Vesselin Kussovski [c], Ivan Angelov [b], Devrim Atilla [a,*]

[a] Gebze Technical University, Department of Chemistry, P.O. Box 141, Gebze, Kocaeli 41400, Turkey
[b] Institute of Organic Chemistry with Centre of Phytochemistry, Bulgarian Academy of Sciences, Acad. G. Bonchev, Bld. 9, 1113 Sofia, Bulgaria
[c] The Stephan Angeloff Institute of Microbiology, Bulgarian Academy of Sciences, Acad. G. Bonchev, Bld. 26, 1113 Sofia, Bulgaria

ARTICLE INFO

Article history:
Received 12 January 2015
Received in revised form 13 March 2015
Accepted 15 March 2015
Available online 17 March 2015

Keywords:
Silicon phthalocyanine
Parabens
Antimicrobial photodynamic therapy
Pathogenic bacteria
Streptococcus mutan

ABSTRACT

A series of silicon(IV) phthalocyanines axially substituted with methylparaben, ethylparaben, propylparaben and butylparaben groups were synthesized and studied as photosensitizers for antimicrobial photodynamic therapy. The absorption, fluorescence, photodegradation and singlet oxygen generation properties of the synthesized Si(IV) phthalocyanines were studied. *In vitro* antibacterial photodynamic therapy was investigated against cariogenic pathogenic bacterium *Streptococcus mutans*. Axially propylparaben substituted Si(IV) phthalocyanine showed significant photodynamic efficacy (log 4) at concentration of 10 μM and mild irradiation (60 mW cm^{-2}, 50 J cm^{-2}, LED 637 nm). The low inactivation capacity was observed for the other studied Si(IV) phthalocyanines. The uptake and localization properties of axially propylparaben substituted Si(IV) phthalocyanine showed a sufficient level of accumulation in planktonic cultured bacterium and a complete penetration depth into the biomass of the 48-h bacterial biofilm.

1. Introduction

Phthalocyanine (Pc) derivatives have a great attention in photodynamic therapy (PDT) of cancer disease as photosensitizers due to their strong absorption in the red visible region, low dark toxicity and high efficiency of singlet oxygen generation [1,2].

Antimicrobial photodynamic therapy (aPDT) is very actual as a promising approach for treatment of resistant pathogenic microorganisms in the so called post-antibiotic era [3,4]. Thus, aPDT has more advantages over the conventional chemotherapeutics such as fast outcome after treatment, safety for human health, lack of the drug resistance and minimal risk for side effects [5]. APDT involves application of non-toxic photosensitizer (PS) in the unexcited state, which after irradiation with red or infrared light (630–850 nm) leads to generation of singlet oxygen and other reactive oxygen species (ROSs) which are toxic to the cells [1,5,6].

Last decade phthalocyanines (Pcs) have been recognized as the most widely studied photosensitizers for photodynamic inactivation of microorganism [3,7] and several studies showed that positively charged Pcs are efficient in the photodynamic inactivation of both Gram-positive and Gram-negative bacteria [8–13]. The number of studies have been published during 90th years of last century concerning differently substituted Si(IV) phthalocyanines for aPDT [14]. Recently Roncucci et al., patented several metal phthalocyanines including silicon(IV) Pcs as antibacterial compositions in 2013. The silicon phthalocyanine (Pc4) has been extensively studied and nowadays Pc4 undergoes phase I for clinical applications [15–17].

Parabens, the alkyl esters of *p*-hydroxybenzoic acid, are one of the most functional preservative agents used in drugs, cosmetics, foodstuffs as well as in dental materials [18,19]. Nevertheless some recent findings of the high level of parabens accumulated in the breast cancer tissues, their negative influence on human health has not been proven and they have been still in usage as additives in the cosmetic products [19–21]. Moreover the restricted applications of parabens in some trademarks assume the development of the alternative antibacterial agents. An effective solution for suppression of bacterial growth is aPDT [22].

* Corresponding author. Tel.: +90 262 6053020.
** Corresponding author. Tel.: +359 9606 181.
E-mail addresses: mantareva@orgchm.bas.bg (V. Mantareva), datilla@gtu.edu.tr (D. Atilla).

http://dx.doi.org/10.1016/j.jphotochem.2015.03.010
1010-6030/

The aPDT is under clinical consideration for treatment of dental caries, which is one of the most common infectious diseases worldwide [6,7,14]. Some results in the literature indicated that parabens are potential antibacterial agents against immobilized or planktonic bacteria found in oral cavity [18]. *Streptococcus mutans* (*S. mutans*) is a Gram-positive bacterium which is mostly found between adjacent teeth or in the deep crevices on the biting surface of teeth [23]. Parabens are known as effective inhibitors of glycolysis in *S. mutans* [19,23]. Experimental aPDT with disulfonated aluminium phthalocyanine has been shown to be effective against biofilms of cariogenic bacteria and against human supragingival dental plaque microbes in the planktonic phase [24].

The present study aims the synthesis of four silicon(IV) phthalocyanines axially substituted with methylparaben, ethylparaben, propylparaben and butylparaben groups. The growth crystals with two of them namely methylparaben- and butylparaben- substituted Si(IV) Pcs were studied. All different parabens substituted Si(IV) Pc were evaluated with their photophysical (absorption and fluorescence) and photochemical (photostability and singlet oxygen generation) properties. The photodynamic effectiveness of the obtained Si(IV) Pcs were investigated against cariogenic bacterium *S. mutans* as planktonic and biofilm cultured.

2. Experimental

2.1. Chemicals

Methanol, tetralin (98%), toluene, tributhylamine and pyridine were obtained from Merck. Tetrahydrofuran (THF) and dimethyl sulfoxide (DMSO) for UV spectroscopy were purchased from Sigma–Aldrich. Toluene and methanol were distilled from sodium benzophenone ketyl and sodium, respectively. Tributhylamine was distilled from CaH_2 and pyridine was distilled from NaOH. All solids were dried under vacuum in such glassware overnight. Thin layer chromatography (TLC) was carry out using Merck precoated silica gel 60 F_{254} TLC plates. The photobiological studies were carried out with the stock solutions of the Si(IV) Pcs which were prepared in concentrations ~2 mM in dimethylformamide (DMF) and stored in the dark and cool place. The dilutions were performed in sterile 0.01 M phosphate-buffered saline (PBS) to 5 and 10 μM final concentrations of the Si(IV) Pcs prior photobiological experiments. The assessment of the drug concentrations was carried out on the basis of the recorded absorption spectra.

2.2. Synthesis

The starting compounds such as 1,3-diiminoisoindoline (**1**) [25–27] and silicon(IV) phthalocyanine dichloride (Si(IV) $PcCl_2$) (**2**) [26] were prepared according to the procedure given in the literature. Synthesis of axially methylparaben substituted silicon(IV) phthalocyanine (**3a**) was published in a Chinese scientific journal [28]. ^{1}H NMR and mass spectra of **3a** were given in Supplementary file as Figs. S5 and S1 respectively.

2.2.1. Phthalocyanine 3b

Silicon(IV) phthalocyanine dichloride (0.5 g, 0.82 mmol), ethyl-4-hydroxybenzoate (1.36 g, 8.18 mmol) and 2 mL dry pyridine in 50 mL dry toluene was refluxed for two days. After evaporation of the solvent in vacuo the residue was dissolved in CH_2Cl_2 and it was purified by preparative thin layer chromatography on silica gel plates using CH_2Cl_2/EtOH (50:1) as eluent to give desired product. The blue colored product was crystalized from chloroform (102 mg, 14.3%). ^{1}H NMR (500 MHz, CD_2Cl_2): δ 9.58–9.60 (m, 8H, Pc-H), 8.34–8.36 (m, 8H, Pc-H), 6.18 (d, J: 7.8 Hz, 4H, p-C_6H_4), 3.76 (q, 4H, OCH_2), 2.38 (d, J: 7.8 Hz, 4H, p-C_6H_4), 0.92 (t, 6H, -CH_3) (Fig. S4 in Supplementary file). Micro TOF-ESI/MS (*m*/*z*) calcd. for $C_{50}H_{34}N_8O_6Si$: 870.94, found: 870.52 $[M]^+$ (Fig. in Supplementary file).

2.2.2. Phthalocyanine 3c

This compound was synthesized according to the procedure described for **3b**. Silicon(IV) phthalocyanine dichloride (0.5 g, 0.82 mmol), propyl-4-hydroxybenzoate (1.47 g, 8.17 mmol) and 2 mL dry pyridine in 50 mL dry toluene to give **3c** as a blue solid (98 mg, 12.9%) ^{1}H NMR (500 MHz, CD_2Cl_2): δ 9.58–9.60 (m, 8H, Pc-H), 8.34–8.36 (m, 8H, Pc-H), 6.19 (d, J: 7.8 Hz, 4H, p-C_6H_4), 3.68 (t, 4H, OCH_2), 2.38 (d, J: 7.8 Hz, 4H, p-C_6H_4), 1.28–1.35 (m, 4H, -CH_2-), 0.63 (t, 6H, -CH_3) (Fig. S6 in Supplementary file). Micro TOF-ESI/MS (*m*/*z*) calcd. for $C_{52}H_{38}N_8O_6Si$: 898.99, found: 921.26 $[M + Na]^+$ (Fig. S5 in Supplementary file).

2.2.3. Phthalocyanine 3d

This compound was synthesized according to the procedure described for **3b**. Silicon(IV) phthalocyanine dichloride (0.5 g, 0.82 mmol), butyl-4-hydroxybenzoate (1.58 g, 8.17 mmol) and 2 mL dry pyridine in 50 mL dry toluene to give **3d** as a blue solid. (105 mg, 13.5%). ^{1}H NMR (500 MHz, CD_2Cl_2): δ 9.58–9.60 (m, 8H, Pc-H), 8.33–8.35 (m, 8H, Pc-H), 6.18 (d, J: 7.8 Hz, 4H, p-C_6H_4), 3.72 (t, 4H, OCH_2), 2.38 (d, J: 7.8 Hz, 4H, p-C_6H_4), 1.25–1.30 (m, 4H, -CH_2-), 1.01–1.09 (m, 4H, -CH_2-), 0.67 (t, 6H, -CH_3) (Fig. S8 in Supplementary file). Micro TOF-ESI/MS (*m*/*z*) calcd. for $C_{54}H_{42}N_8O_6Si$: 927.05, found: 949.29 $[M + Na]^+$ (Fig. S7 in Supplementary file).

2.3. Equipment

NMR spectra were recorded on Varian 500 MHz spectrometer using the deuterated CD_2Cl_2. Electrospray ionization (ESI) mass spectrometry was carried out on Bruker Micro TOF-ESI/MS spectrometer. Absorption spectra were recorded on Shimadzu 2101 UV–vis spectrophotometer. The fluorescence studies were performed with Varian Eclipse and Fluorolog-3 fluorimeters. The bacterial biofilm was examined with confocal laser scanning microscope (CLSM) of Leica Microsystems (Model: Leica TCS SPE) with Leica LAS AF software. General Electric quartz line lamp (300 W) was used for photoirradiations studies. A 600 nm glass cut off filter (Schott) and a water filter were used to filter off ultraviolet and infrared radiations, respectively. An interference filter (Into, 670 nm for **3a**–**d** with a band width of 40 nm) was additionally placed in the light path before the sample. Light intensities were measured with a POWER MAX5100 (Molelectron detector incorporated) power meter.

2.4. Photophysical and photochemical parameters

2.4.1. Fluorescence quantum yields

Fluorescence quantum yields (Φ_F) were determined in DMF by the comparative method using Eq. (1) [29,30],

$$\Phi_F = \Phi_F(\mathrm{Std}) = \frac{F_{Std} A_{Std} n^2}{F_{Std} A n_{Std}^2} \quad (1)$$

where F and F_{Std} are the areas under the fluorescence emission curves of the samples (**3a**–**d**) and the standard, respectively. A and A_{Std} are the respective absorbances of the samples and standard at the excitation wavelengths and n and n_{std} are the refractive indices of solvents used for the sample and standard, respectively. Unsubstituted ZnPc (Φ_F = 0.20) [31] was employed as the standard in DMSO.

2.4.2. Singlet oxygen quantum yields

Singlet-oxygen quantum yield (Φ_Δ) determinations were carried out using the experimental setup described in the

literature [30,32]. Typically, a 2 mL portion of the respective axially paraben substituted silicon(IV) phthalocyanine (**3a–d**) solutions ($C = 1.00 \times 10^{-5}$ M) that contained the singlet oxygen scavenger was irradiated in the Q-band region with the photoirradiation setup described in the literature [30,32]. The Φ_Δ values were determined in air using the relative method with 1,3-diphenylisobenzofuran (DPBF) as a singlet oxygen chemical scavenger in DMF using Eq. (2).

$$\Phi_\Delta = \Phi_\Delta^{Std} \frac{RI_{abs}^{Std}}{R^{Std} I_{abs}} \quad (2)$$

Φ_Δ^{Std} is the singlet oxygen quantum yield for the standard unsubstituted ZnPc ($\Phi_\Delta^{Std} = 0.56$ in DMF) [33]. R and R_{Std} are the DPBF photobleaching rates in the presence of the respective axially paraben substituted silicon(IV) phthalocyanine (**3a–d**) and standard, respectively; I_{abs} and I_{abs}^{Std} are the rates of light absorption by the samples (**3a–d**) and standard, respectively. The concentrations of DPBF in the solutions were calculated using the determined value of $\log\varepsilon = 4.36$ at 417 nm in DMF. The light intensity used for Φ_Δ determinations was found to be 6.58×10^{15} photons s^{-1} cm^{-2}.

2.4.3. Photodegradation quantum yields

Photodegradation quantum yield (Φ_d) determinations were carried out using the experimental set-up described in literature [30,32]. Photodegradation quantum yields were determined using Eq. (3),

$$\Phi_d = \frac{(C_0 - C_t)VN_A}{I_{abs} S t} \quad (3)$$

where C_0 and C_t are the samples (**3a–d**) concentrations before and after irradiation respectively, V is the reaction volume, N_A is the Avogadro's constant, S is the irradiated cell area, t is the irradiation time and I_{abs} is the overlap integral of the radiation source light intensity and the absorption of the samples (**3a–d**). A light intensity of 2.19×10^{16} photons s^{-1} cm^{-2} was employed for Φ_d determinations.

2.5. X-ray crystallography

Intensity data were recorded on a Bruker APEX II QUAZAR diffractometer using monochromatized Mo Kα X-radiation (λ = 0.71073 Å). Absorption correction was performed by multi-scan method implemented in SADABS [34] and space groups were determined using XPREP implemented in APEX2 [35]. Structures were determined using the direct methods procedure in SHELXS-97 and refined by full-matrix least squares on F^2 using SHELXL-97 [36]. All non-hydrogen atoms were refined with anisotropic displacement factors. The C–H hydrogen atoms were placed in calculated positions and the displacement parameters of the H atoms were fixed at $U_{iso}(H) = 1.2U_{eq}$ of their parent atoms. The final geometrical calculations were carried out with PLATON [37], and MERCURY [38] programs and the molecular drawings were done with DIAMOND [39] program. Structure determinations have been deposited with the Cambridge Crystallographic Data Centre with references CCDC 976697 and 976698 for compounds **3a** and **3d**, respectively.

2.6. Antimicrobial photodynamic therapy

2.6.1. Bacterial strain

The Gram-positive cariogenic bacterium *S. mutans* strain 20523 from the collection DSMZ – Germany was used for antimicrobial PDT studies. The bacteria were incubated in microaerophilic conditions (5% CO_2) at 37 °C for 48 h on solid medium Trypticase® Soy agar, supplemented with 0.3% yeast extract.

2.6.2. Biofilm assay

Biofilm assay was performed on coverslips, which were placed in commercial presterilized polystyrene flat bottomed 12-well cell culture test plates (Switzerland). A standard bacterial suspension (1 mL, 10^7 CFU mL^{-1}) prepared after serial dilutions was applied onto the surface of the discs placed in each well of the plate followed by incubation for 1.5 h at 37 °C to promote cellular adherence to surface of the discs. The blank control wells with the discs at the same conditions but without bacterial cells were inoculated. After the initial adhesion phase, the cell suspensions were aspirated and the discs were gently washed with PBS to remove loosely adherent cells. In the biofilm phase formation of *S. mutans* an addition of 4 mL Tryptic soy broth (Difco Laboratories, MD, USA) was placed in each well. The plates were covered and incubated for 48 h at 37 °C to form the microbial biofilm for *in vitro* experiments.

2.6.3. In vitro *photodynamic study*

Bacterial suspensions (1 mL) were incubated with the axially parabens substituted SiPcs (**3a–3d**) for 15 min, by using the freshly prepared stock solutions in DMF (0.5% DMF from the total volume) with two different concentrations after dilution (5.0 μM and 10 μM SiPcs). The incubation was carried out on magnetic stirrer in the dark at room temperature. The bacterial suspensions were with cell densities between 10^6 and 10^7 CFU mL^{-1} in PBS. After incubation time was passed an aliquot (200 μL) of the suspension was placed in a standard palette where the irradiation was performed. The samples were irradiated with a LED 637 nm with fluence rate 60 mW cm^{-2} and total light dose 50 J cm^{-2}. The power density was controlled with photometer before and after irradiation. The biofilm of bacteria cells developed for 48-h incubation at 37 °C by using coverslips were washed with PBS and were incubated with 5 μM and 10 μM SiPcs for 1.5 h in dark place. The samples were washed again after incubation and were positioned for irradiation with 637 nm. The samples of four control groups were collected: (1) with SiPc, but no light (dark toxicity), (2) without SiPc, but illuminated, (3) only bacterial suspension (no SiPc, no light) and (4) bacteria incubated with DMF (5% from the total volume). After irradiation, the aliquot of cells (0.1 mL) was taken off and serially diluted (10-fold) with PBS. The same action was repeated for the control samples (1–4). Aliquots (0.1 mL) were spread over Trypticase® Soy agar. The number of colonies (CFU) on each plate was counted following 48 h incubation at 25 °C.

2.6.4. Uptake study

The uptake study was carried out with four axially paraben substituted Si(IV) Pc (**3a–3d**) by using a previously described chemical extraction procedure [9]. The quantification of the number of the sensitizer molecules accumulated into *S. mutans* cells was carried out by the means of fluorescence measurements of the collected samples. The estimation of the uptake for 5 μM 3a–3d into bacterial cells after 15 min incubation in the dark was carried out for the cellular suspensions with different densities (10^5–10^8 CFU mL^{-1}). The collected samples for fluorescence measurements were as followed: (1) the supernatant of phosphate buffered saline (PBS) after incubation, (2) the PBS after first and (3) after second cell wash and (4) THF: 2% SDS (9:1) solution after cellular extraction. The collected samples (1–4) were diluted with THF and measured at excitation wavelength 637 nm. All measurements were carried out by using previously described set-up for fluorescence measurements [40]. The results were presented as number of the photosensitizer molecules per one cell by processing the obtained values of fluorescence intensities and

referring to the calibration curves taken for SiPc (3a–3d) in the solvent mixtures used for fluorescent measurements.

2.6.5. Confocal laser scanning microscopy

The biofilms of *S. mutans* developed for 48 h incubation at 37 °C on coverslips were used for study of penetration depth and localization of SiPcs. The biofilm images were processed via the Leica LAS AF software provided with the CLSM as previously described in Ref. [41]. The oil immersion of 63× objective (NA = 1.23) was used. The bacterial biofilms were characterized with a BacLight Live-Dead bacterial viability kit, L13152 (Molecular Probes, Europe BV). The kit contains two fluorescence stains: SYTO9 and propidium iodide. The preparation and application of the dyes were according to the product information list. The viable cells were detected by fluorescence from the SYTO9 stain (exc. 488 nm, em: 525 nm). The dead cells were detected by fluorescence from the propidium iodide (exc: 520 nm, em: 620 nm). The images of a 0.150 μm slices were taken by scanning the biofilms of bacterial specie (*S. mutans*). The thickness of biofilm was evaluated by the native fluorescence of bacterial cells (exc. 488 nm, em. 520–580 nm). The biofilm was incubated for 1.5 h with SiPc then after washing in PBS it was covered with a coverslip. The fluorescence of Si(IV) Pcs inside the biofilm was imaged by excitation with 633 nm laser and emission between 660 and 740 nm to observe the phthalocyanine penetration depth into biomass. The whole biofilm was scanned on slices of 0.150 μm following the red fluorescent signal as well as the auto fluorescence. The co- localization of dye into the biomass was evaluated.

2.6.6. Statistics

The uptake and *in vitro* photoinactivation experiments were carried out in triplicate and the data were presented as a mean ± standard deviation (SD). The difference between two means was compared by two-tailed unpaired Student's test. The values of $P < 0.05$ were considered as significant.

3. Results and discussions

3.1. Synthesis and characterization

The synthesis of the target compounds involves the nucleophilic displacement of two chlorides substituents from $SiPc(Cl)_2$ by reaction of paraben derivatives in dried toluene and pyridine at reflux temperature. Synthetic pathway for the synthesis of axially di-parabens substituted Si(IV) phthalocyanines (**3a**–**3d**) was presented in Scheme 1. The proposed structures of newly synthesized Si(IV) phthalocyanine derivatives (**3b**–**3d**) were confirmed by ^{1}H NMR spectra. ^{1}H NMR spectra of the axially-paraben substituted Si(IV) Pcs showed intense multiple signals at around δ9.5 and 8.3 ppm belonging to the aromatic Pc ring protons. The close proximity of the ligands to the Pc ring delocalization induced large up-field shifted resonances for the ligand protons. Thus four aromatic hydrogen atoms belonging to ligands gave a doublet at around δ 2.4 ppm for **3b**–**3d**. The novel Si(IV) phthalocyanine derivatives were also characterized by ESI/MS mass spectroscopy. Molecular ion peaks were compatible with calculated values for **3b**–**3d.** Mass (Figs. S3, S5 and S7) and ^{1}H NMR (Figs. S4, S6 and S8) spectra of compounds **3b**–**3d** were given in the supplementary file. IR spectra of **3b–3d** were also confirmed the proposed structures.

3.2. X-ray crystallography of the axially paraben substituted Si(IV) phthalocyanines

The crystal structures of **3a** and **3d** were determined by X-ray crystallography. The data collection and refinement details were given in Table 1. **3a** had triclinic system, *P-1* space group while **3d**

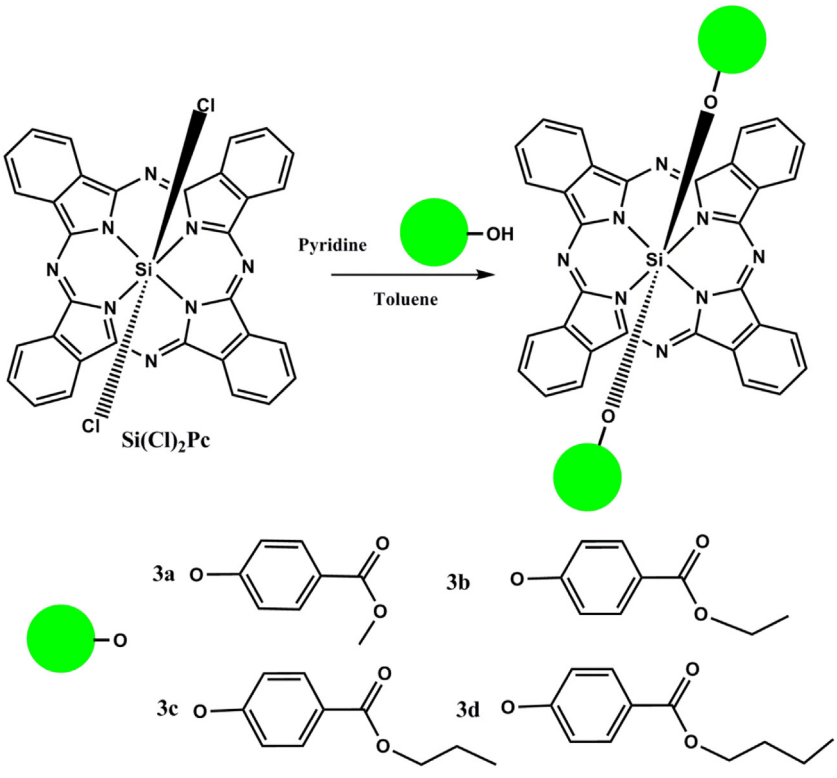

Scheme 1. Synthetic pathway for the preparation of silicon(IV) phthalocyanines axially substituted with different paraben groups.

Table 1
X-ray crystallographic data and refinement parameters for the compounds **3a** and **3d**.

Compound	3a	3d
Empirical formula	$C_{48}H_{30}N_8O_6Si$	$C_{54}H_{42}N_8O_6Si$
Formula weight	842.89	927.05
Temperature (K)	120(2)	120(2)
Crystal system	Triclinic	Orthorhombic
Space group	*P-1*	*Pbca*
a (Å)	7.6630(13)	21.979(9)
b (Å)	10.8722(19)	8.501(4)
c (Å)	12.013(2)	23.726(10)
α (°)	104.948(9)	
β (°)	94.127(10)	
γ (°)	98.972(10)	
Volume (Å^3)	948.5(3)	4433.(3)
Z	1	4
Density (calc, Mg/m^3)	1.476	1.389
Absorption coeff. (mm^{-1})	0.130	0.118
F(000)	436	1936
θ_{max} (°)	28.37	25.02
Reflections collected	16928	29828
Independent reflections	4700	3903
R_{int} (merging *R* value)	0.0386	0.1045
Data/Restrains/Parameters	4700/0/287	3903/0/314
R ($F^2>2\sigma F^2$)	0.0416	0.0523
wR (all data)	0.1095	0.1276
Goodness-of-fit on F^2	1.028	1.066

had orthorombic system, *Pbca* space group. Although **3a** was synthesized previously [28], its crystal structure was given in this study.

In structures, the phthalocyanine molecule sit on an inversion centre (Fig. 1) and Si atom which laid on a centre of symmetry was six-coordinate with four inner nitrogen atoms on Pc core and two oxygen atoms on the paraben's units in an octahedral environment. The Pc rings of both structures were essentially planar and the SiN_4 coordination was perfectly square planar, the N1—Si—N2 bond angles were nearly perpendicular [*av.* 90,00 (±0.55)°] while the N1—Si—N1# and the N2—Si—N2# bond angles were linear with 180,00 (7)°. The O—Si—O bond angles were also linear [18.000(6)°], and the angle between the main plane of Pc ring and benzyl ring of axially substituted paraben derivative was 49,29° in **3a** and 45,85° in **3d** (Fig. depicted S9 in the supporting file). The Si-N [*av.* 1910(±0.002) Å for **3a** and 1908 (±0.016) Å for **3d**] and the Si—O [1.7315(10) Å for **3a** and 1,7168 (19) Å for **3d**] bond lengths were compatible with those previously observed for the similar SiPc derivatives which were axially substituted with several alkoxy groups [42–44] (The selected bond and conformational parameters were given in Table S1 in the supporting file).

The crystal packing investigations of **3a** and **3d** showed that there was no classic hydrogen bonds in both unit cells, but there were several C—H···π and π–π intermolecular interactions which were stabilizing the packing of both unit cells, the selected intermolecular interactions (<4.0 Å) were listed in Table S2. In a unit cell of **3a**, there were additionally two different kinds of intermolecular C—H···O interactions between the ester oxygen atoms of paraben groups and phthalocyanine rings less than 3.5 Å and the phthalocyanine rings were packed vertically (Fig. S10). In the case of **3d**, these interactions were not observed probably due to longer alkyl chain (*n*-butyl), instead the intermolecular C—H···N interaction was observed. Therefore, the phthalocyanine rings were packed in the zigzag chain-like arrangement along *a* axis (Fig. S11).

3.3. UV–vis absorption and fluorescence properties

Four studied axially paraben substituted Si(IV) phthalocyanines (**3a**–**3d**) were soluble in most of organic solvents such as toluene, tetrahydrofuran, dichloromethane, chloroform and *N*,*N*-dimethylformamide and partly in DMSO. Electronic absorption spectra of the **3a**–**3d** were measured in the above solvents and the Q-bands were observed with maxima at around 680 nm (Table 2). The B bands were also observed at around 355 nm. The sharp Q-bands observed in all studied solvents were an evidence of the formation

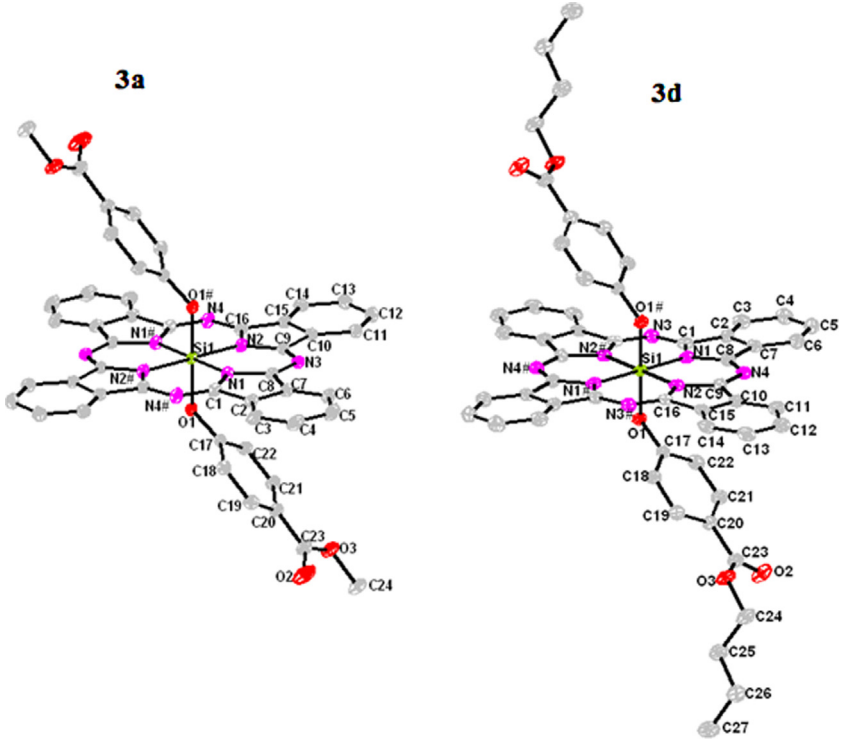

Fig. 1. Crystal structures of compounds **3a** and **3d** with the atom-numbering scheme. Displacement ellipsoids were drawn at the 50% probability level. The hydrogen atoms have been omitted for clarity (Symmetry code{#} for **3a:**-x + 1, -y + 1, -z; for **3d:** -x, -y + 1 -z + 1).

Table 2
Absorption, excitation and emission spectral data for the axially parabens substituted silicon (IV) phthalocyanine in DMF.

Compound	Q band λ_{max}, (nm)	log ε	Excitation λ_{Ex}, (nm)	Emission λ_{Em}, (nm)	Stokes shift Δ_{Stokes}, (nm)
3a	683	5.10	684	690	6
3b	682	5.16	685	690	5
3c	683	5.29	684	690	6
3d	682	5.35	683	690	7
ZnPc[a]	670	5.37	670	676	6

[a] Data from Ref. [33].

of non-aggregated species. The further photophysical and photochemical studies were performed in DMF. Fig. 2 showed the electronic absorption spectra of **3a–3d** in DMF at the concentration of 10^{-5} M. The absorption intensities and extinction coefficients of the studied phthalocyanines grow bigger with the growth of the hydrocarbon length on the paraben groups (Fig. 2 and Table 2). The hydrocarbon length did not show any effect on the maxima of absorption wavelength of these compounds.

All studied phthalocyanines showed similar fluorescence emission spectra in DMF. Fig. 3 showed the absorption, fluorescence emission and excitation spectra of compound **3d** as an example in DMF. Fluorescence emission and excitation maxima of **3a–3d** in DMF were listed in Table 2. All studied Si(IV) phthalocyanines showed the same fluorescence emission maxima (690 nm) in DMF. The observed Stokes shifts for **3a–3d** were similar with unsubstituted zinc phthalocyanine used as a standard compound (Table 2).

The excitation spectra of axially paraben substituted silicon(IV) phthalocyanines (**3a–3d**) were related to absorption spectra and both were mirror images of the fluorescence spectra in DMF (Fig. 3). The proximity of the wavelength in absorption and excitation spectra of each component indicated that the nuclear configurations of the ground and excited states are similar and not affected by the excitation wavelength for all studied compounds.

The phthalocyanines possess an optimal fluorescence behavior which is suitable for imaging of the studied object. The fluorescence properties such as fluorescence quantum yield (Φ_F) and fluorescence lifetime (τ_F) are also important for PDT applications. The fluorescence quantum yields (Φ_F) of **3a–3d** were determined in DMF and they showed similar Φ_F values (Table 3) which were higher than that of unsubstituted Zn(II) phthalocyanine. The increase in the hydrocarbon chain length did not show any significant effect on the Φ_F values.

The fluorescence decay curves of **3a–3d** were recorded for excitation wavelength of 405 nm and resulted in two exponential curves of life-times (τ_F) in DMF (Fig. 4A). This observation could be explained with the ability of **3a–3d** to form non-fluorescent species at concentrations over 10^{-5} M in DMF. It was well observed that the ground-state dimers were the physical quenchers for the monomeric molecules in the excited state [45]. The obtained two life-times with a difference of two orders of magnitude measured in DMF suggested the formation of physical aggregates (Fig. 4A). The contribution of the shorter life-time component evaluated from the fluorescence decay curves was about 96 ± 1% and the measured life-times were between 5.6 and 7.1 ns. The mono-exponential curves with life-times between 5.8 and 6.2 ns were obtained for studied phthalocyanines **3a–3d** in THF (Fig. 4B). The life-time values were similar without dependence on the hydrocarbon chain of the substituted parabens. A mono-exponential curve was also observed for the axially hydroxyl substituted SiPc (τ_F = 5.4 ns in THF) used as a reference compound. The obtained values decreased with 0.2–0.3 ns for excitation with a picosecond diode at 654 nm. The values of the excited state life-times of **3a–3d** in DMF as compared to τ_F in THF showed an essential increasing for SiPc **3a**. The value of τ_F was 1.5 ns higher in DMF than that in THF (5.6 ns). The obtained values of life-time of fluorescence were of the same order of magnitude for the other three axially paraben substituted Si(IV) phthalocyanines (**3b–3d**). The obtained values were not dependent on the excitation neither the observation wavelengths.

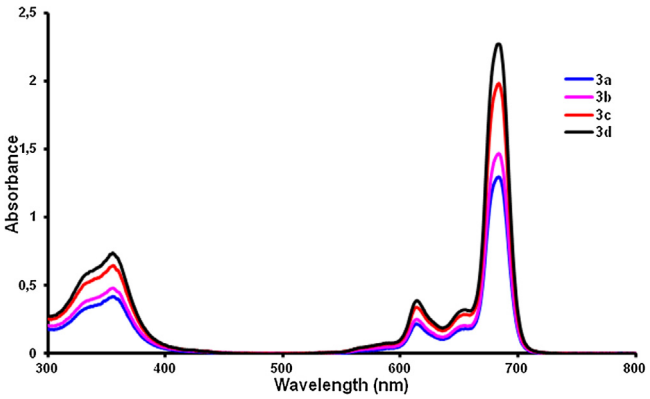

Fig. 2. Absorption spectra of **3a–3d** in DMF at the concentration of 10^{-5} M.

3.4. Singlet oxygen study

The formed singlet oxygen in the presence of axially paraben substituted silicon(IV) phthalocyanines was determined by following the chemical method based on the chemical quenching of 1,3-diphenylisobenzofuran (DPBF). The intensity of DPBF absorbance at 417 nm decreased with light irradiation (Fig. 5). The intensities of Q bands for **3a–3d** did not show any change indicating that the photodegradation did not occur by the light exposure during the singlet oxygen studies. The studied **3a–3d** showed similar Φ_Δ values (around 0.50) which were slightly lower than unsubstituted Zn(II) phthalocyanine (Table 3). The Φ_Δ values of the studied paraben substituted Si(IV) Pcs were found with higher Φ_Δ value than for axial hydroxyl substituted Si(IV) Pc in DMSO (Φ_Δ = 0.28) [46]. The increasing of the hydrocarbon chain from **3a** to **3d** did not show any quenching effect on singlet oxygen generation.

Table 3
Photophysical and photochemical data for the axially parabens substituted silicon (IV) phthalocyanines in DMF.

Compound	Φ_F	Φ_d (x10^{-5})	Φ_Δ
3a	0.30	6.29	0.47
3b	0.27	0.18	0.47
3c	0.27	0.15	0.46
3d	0.27	0.13	0.48
ZnPc[a]	0.17	2.3	0.56

[a] Data from Ref. [33].

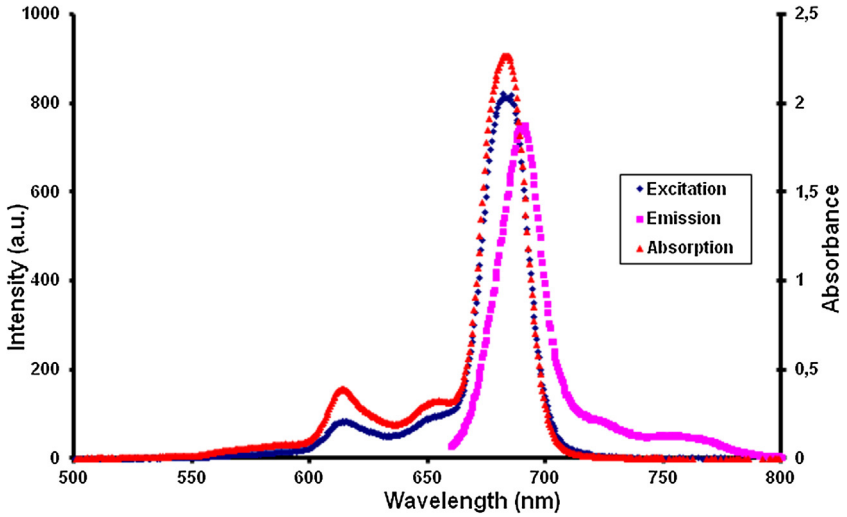

Fig. 3. Absorption, excitation and emission spectra of **3d** in DMF (λ_{exc}: 650 nm).

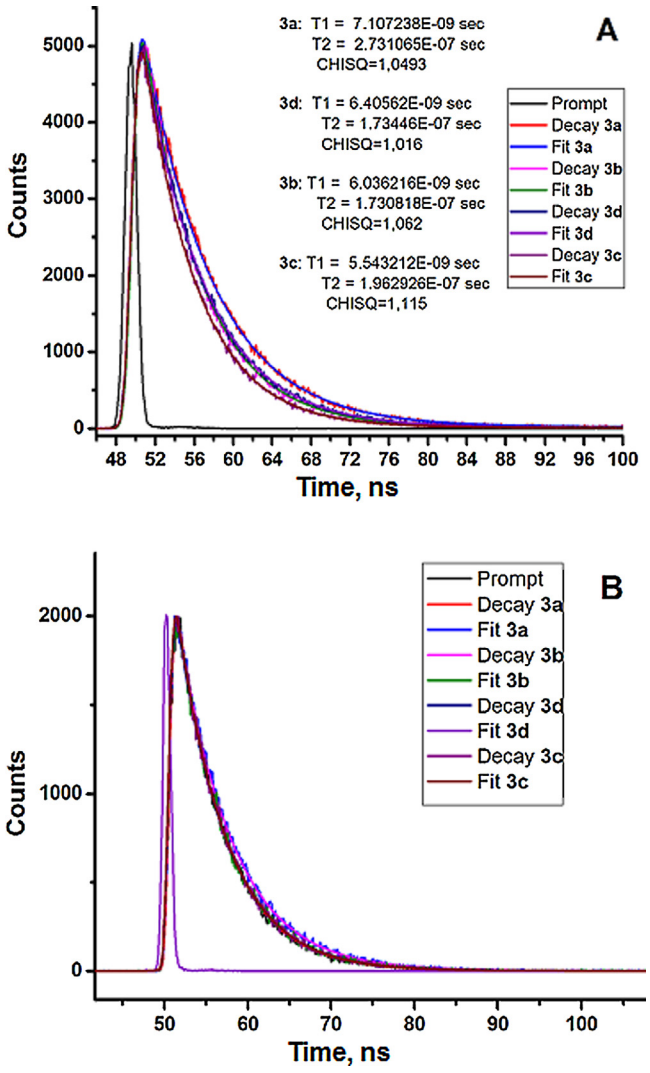

Fig. 4. Time-resolved fluorescence of the compounds **3a–3d** in DMF (**A**) and THF (**B**). λ_{exc}: 405 nm.

3.5. Photostability study

The photodegradation of **3a–3d** under light irradiation was defined by the photodegradation quantum yield (Φ_d). The decreasing of the absorption bands for the DMF solutions of the studied phthalocyanines were determined by UV–vis spectroscopy. The observed spectral changes were shown as an example for phthalocyanine **3c** in DMF (Fig. 6). The obtained Φ_d values were presented in Table 3. Generally, Φ_d values of the studied silicon(IV) Pc compounds were lower than unsubstituted zinc(II) phthalocyanine except for **3a**. The Φ_d value for **3a** was higher than for the other studied silicon(IV) phthalocyanines as well as unsubstituted zinc(II) phthalocyanine.

3.6. In vitro *studies*

The photodynamic inactivation studies with axially methylparaben, ethylparaben, propylparaben and butylparaben substituted Si(IV) Pcs towards *S. mutans* in suspension (10^6 CFU mL^{-1}) were presented in Fig. 7. Si(IV) Pcs showed the lack of dark toxicity against planktonic cultured *S. mutans* at concentrations of 5 μM and 10 μM. The dark toxicities due to the length chains of different alkyl- parabens were not observed. Among four studied photosensitizers **3a–3d**, the photoinactivation was significant only after treatment with **3c**. The other three Si(IV) Pcs (**3a**,**3b** and **3d**)

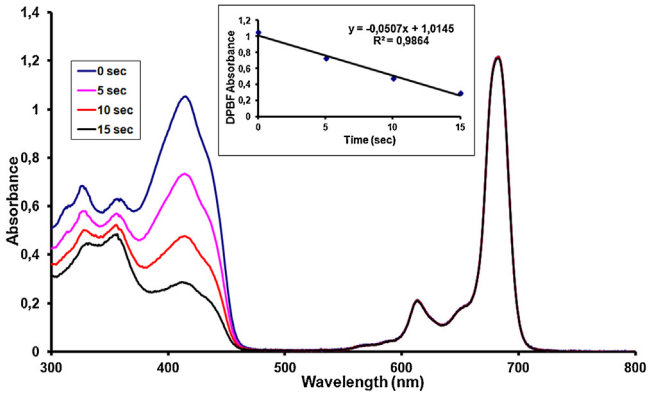

Fig. 5. Absorption changes due to photobleaching of DPBF obtained by irradiation of **3d** at a concentration of 10^{-5} M for determination of the produced singled oxygen (Inset: Plot of DPBF absorbance versus time).

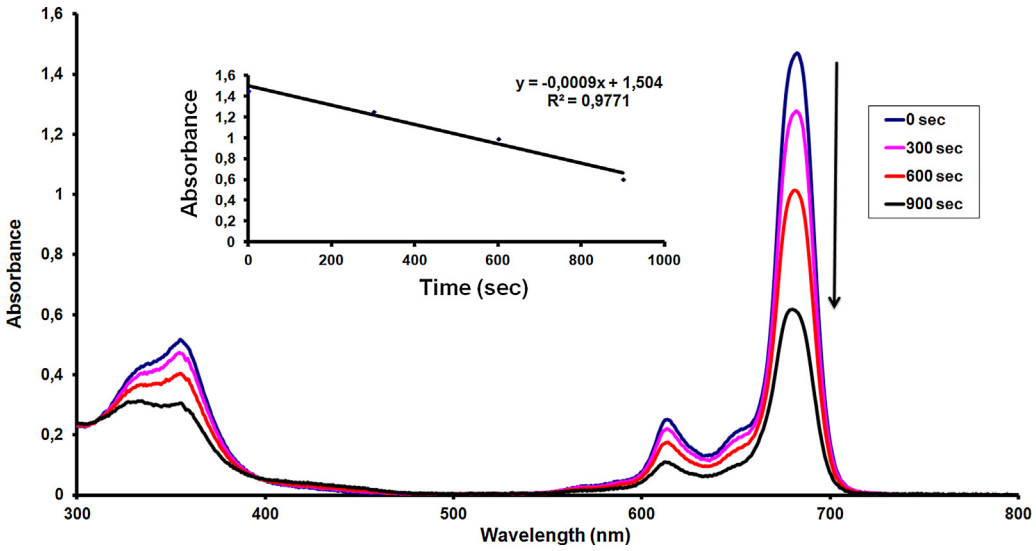

Fig. 6. Absorption changes during the photodegradation studies of the compound **3c** in DMF. (Inset: Plot of the Q band decrease of absorbance versus time). 300 W General electric quartz line lamp with power density of 18 mW/cm^2 was used as a light source.

showed lower photodynamic efficacy (<log 3) at the applied concentrations (5 μM and 10 μM).

The comparison of the axial propylparaben substituted Si(IV) Pc **3c** with the recently studied tetra-methylpyridyloxy substituted Si (IV)-phthalocyanine (SiPcMe) [47] suggested the higher photo-inactivation efficiency for the newly studied Si(IV) Pc. It was found that the bacterial cells were photoinactivated approximately 1 log at the same experimental conditions. Nevertheless the lower uptake of **3c** as compared to cationic SiPcMe, compound **3c** was with high photocytotoxicity towards *S. mutans* planktonic cells.

The *in vitro* experiments on 48-h biofilms showed low ability for photoinactivation even with the active Si(IV) Pc **3c** at the used PDT protocol, namely concentrations up to 10 μM, prolong incubation time (1.5 h) and gentle irradiation from a LED 637 nm. In our previous works with SiPcMe the effect was also negligible towards most of the treated bacterial strains at different photodynamic therapeutic conditions [47–49].

3.7. Uptake study

The uptake study was performed with photodynamically effective propylparaben SiPc **3c** as well as for **3a**, **3b** and **3d**with *S. mutans* as planktonic cultured (Fig. 8). The spectra were recorded in the spectral range 650–800 nm at excitation wavelength of therapeutic light 637 nm by using set-up for fluorescence measurements, which was described in our previous papers [40,41]. It was found an inverse behavior of the decreasing accumulation of **3a–3d**the SiPcs with increase of the cell densities of suspensions (10^5–10^8 CFU mL^{-1}). The calculated amount of **3a–3d** into bacterial cells was estimated between 20% and 30% from the total amount of the incubated photosensitizer. The incubation was performed for 15 min than the cells were washed to remove the non-bounded compound in order to estimate the real level of saturation.

A high number of the bound **3c** molecules per one bacterial cell at lower cell density were in the agreement with our previous findings and the literature [9,50,51]. The uptake study with propylparaben Si(IV) Pc suggested that the accumulation of a photosensitizer into cells at low cell density will have a substantial effect on the photodynamic response. The phenomenon of an inverse dependence of the number of dye molecule on the cell density was firstly reported by Demidova and Hamblin for photodynamic sensitizer and *Escherichia coli* bacterial cells [50]. The chemical structure of the photosensitizer, as the experimental conditions (incubation time, temperature and concentration) is a key factor for the uptake and further photodynamic effect [33]. The

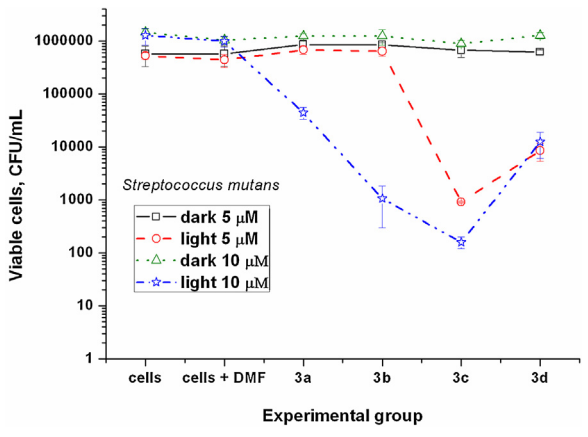

Fig. 7. Survival of *S. mutans* cells (10^6 cells mL^{-1}) incubated with 5 μM and 10 μM **3a–3d** for 15 min and irradiated with LED 637 nm with a light dose 50 J cm^{-2}.

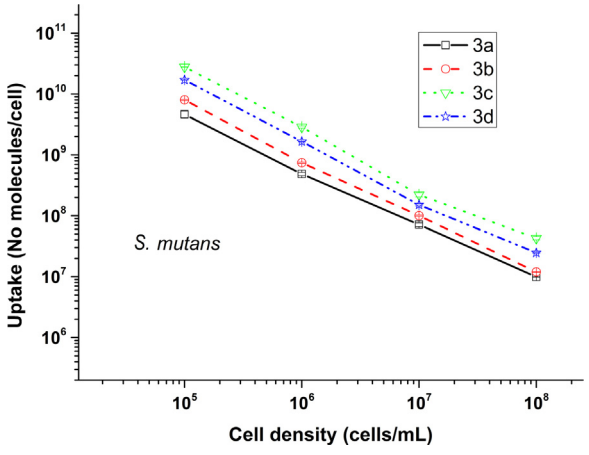

Fig. 8. Uptake of 10 μM Si(IV) Pc 3a–3d after 15 min incubation of *S. mutans* cell suspension with different cell densities.

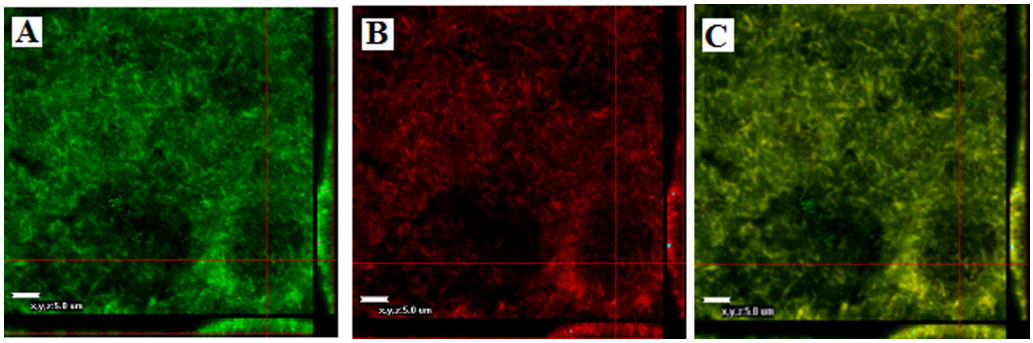

Fig. 9. Confocal laser scanning fluorescence images of *S. mutans* biofilm taken at (**A**) λ_{exc}: 488 nm, λ_{em}: 520–580 nm (green autofluorescence) and (**B**) λ_{exc}: 633 nm and λ_{em}: 660–740 nm (red fluorescence of **3c**) and (**C**) overlap of both images. Magnification x63.

optimal incubation time was observed to be between 5 and 30 min for an optimal level of uptake of a non-charged phthalocyanine [51]. It is well studied that the binding process occurs as a result of compound hydrophobicity or by an electrostatic mechanism of interactions [50,51]. The studied Si(IV) Pcs are non-charged photosensitizer with hydrophobic nature, which appears favorable property for penetration into lipophilic cell membrane.

3.8. Localization of **3c** in bacterial biofilm

The bacterial biofilm was developed on coverslips and was characterized by the native fluorescence of the cell chromophores (λ_{exc}: 488 nm; λ_{em}: 500–580 nm) by a laser scanning of the biofilm (Fig. 9A). The visualization of red fluorescence of phthalocyanine dye (λ_{exc}: 633 nm, λ_{em}: 660–740 nm) was obtained for the slices of biofilm with thickness of 0.150 μm (Fig. 9B). In addition z-axis was pictured for determination of the biofilm thicknesses (4–5 μm) and the penetration depth of compound **3c** into the whole biomass. The obtained bright fluorescence signal and co-localization image shown in Fig. 9C suggested that Si(IV) Pc **3c** was localized inside the bacterial cells, but not in the matrix (Fig. 9A–C, dark area). The assessments of the penetration depth were performed by the fluorescence mode as well as the transmission mode which suggested that **3c** was distributed into the whole biomass. In case of bacterial biofilm formed for 48-h, it needed longer incubation time (1.5 h) than the time (5–30 min) necessary for dye uptake in cell suspension [4,9,41]. Under the used treatment conditions, SiPc **3c** was rapidly bound to *S. mutans* cells with full penetration into the formed 48-h biofilm (~5 μm) as observed by the confocal fluorescence microscopy studies.

4. Conclusions

Four axially-paraben substituted silicon(IV) phthalocyanines were synthesized and their photophysical and photochemical properties were studied. The hydrocarbon chain of the axial groups (methyl-, ethyl-, propyl, butyl- paraben) did not show any effect on the absorption and fluorescence spectra, and singlet oxygen characteristics, but slightly influence on the extinction coefficients and quantum yield of photodegradation (Φ_d). The fluorescence quantum yields (Φ_F) of the axially paraben substituted Si(IV) Pcs were higher than unsubstituted Zn(II) Pc. The new Si(IV) Pcs showed the similar singlet oxygen quantum yields ($\Phi_\Delta \sim 0.50$) which was slightly lower than unsubstituted Zn(II) phthalocyanine but the observed Φ_Δ values for newly synthesized axially paraben substituted Si(IV) Pcs were found higher than the Φ_Δ value of Si(IV) Pc with axial ligands of two OH groups. Among the studied four Si (IV) Pcs the propylparaben- Si(IV) Pc was with an optimal antimicrobial PDT efficiency which can be result of the appropriate uptake into cell membrane and sufficient singlet oxygen generation able to inactivate bacterial cells. The different alkyl groups to Si(IV) were not contributed to the inactivation capacity of the studied axial paraben substituted SiPcs towards bacterium strain *S. mutans*.

Acknowledgements

This work was supported by the collaboration project between Scientific and Technological Research Council of Turkey (TUBITAK) Project No: 212M053 and Bulgarian Academy of Sciences and partly by the National Science Fund, Bulgaria (B02/9/2014).

Appendix A. Supplementary data

Supplementary data associated with this article can be found, in the online version, at http://dx.doi.org/10.1016/j.jphotochem.2015.03.010

References

[1] E.A. Lukyanets, Phthalocyanines as photosensitisers in the photodynamic theraphy of cancer, J. Porphyrins Phthalocyanines 3 (1999) 424–432.
[2] C.M. Allen, W.M. Sharman, J.E. van Lier, Current status of phthalocyanines in the photodynamic theraphy of cancer, J. Porphyrins Phthalocyanines 5 (2001) 161–169.
[3] N. Nombona, E. Antunes, W. Chidawanyika, P. Kleyi, Z. Tshentu, T. Nyokong, Synthesis, photophysics and photochemistry of phthalocyanine-ε-polylysine conjugates in the presence of metal nanoparticles against *Staphylococcus aureus*, J. Photochem. Photobiol. A 233 (2012) 24–33.
[4] V. Mantareva, I. Angelov, D. Wöhrle, E. Borisova, V. Kussovski, Metallophthalocyanines for antimicrobial photodynamic therapy: an overview of our experience, J. Porphyrins Phthalocyanines 17 (2013) 399–416.
[5] M. Wainwright, Photodynamic antimicrobial chemotherapy (PACT), J. Antimicrob. Chemother. 42 (1998) 13–28.
[6] X. Fu, Y. Fang, M. Yao, Antimicrobial photodynamic therapy for methicillin-resistant *Staphylococcus aureus* infection, BioMed. Res. Int. (2013) Article ID 159157.
[7] T.N. Demidova, M.R. Hamblin, Photodynamic therapy targeted to pathogens, Int. J. Immunopathol. Pharmacol. 17 (2004) 245–254.
[8] M. Cormick, M. Rovera, E. Durantini, Synthesis, spectroscopic properties and photodynamic activity of a novel Zn(II) phthalocyanine substituted by fluconazole groups, J. Photochem. Photobiol. A 194 (2008) 220–229.
[9] V. Mantareva, V. Kussovski, I. Angelov, E. Borisova, L. Avramov, G. Schnurpfeil, D. Wöhrle, Photodynamic activity of water-soluble phthalocyanine zinc(II) complexes against pathogenic microorganisms, Bioorg. Med. Chem. 15 (2007) 4829–4835.
[10] A. Segalla, C.D. Borsarelli, S.E. Braslavsky, J.D. Spikes, G. Roncucci, D. Dei, G. Chiti, G. Jori, E. Reddi, Photophysical, photochemical and antibacterial photosensitizing properties of a novel octacationic Zn(II)-phthalocyanine, Photochem. Photobiol. Sci. 1 (2002) 641–648.
[11] I. Scalise, E. Durantini, Synthesis, properties, and photodynamic inactivation of *Escherichia coli* using a cationic and a noncharged Zn(II) pyridyloxyphthalocyanine derivatives, Bioorg. Med. Chem. 13 (2005) 3037–3045.
[12] M. Spesia, M. Rovera, E. Durantini, Photodynamic inactivation of *Escherichia coli* and *Streptococcus mitis*by cationic zinc(II) phthalocyanines in media with blood derivatives, Eur. J. Med. Chem. 45 (2010) 2198–2205.

[13] D. Wöhrle, S. Muller, M. Shopova, V. Mantareva, G. Spassova, F. Vietri, F. Ricchelli, G. Jori, Effect of delivery system on the pharmacokivetic and phototherapeutic properties of bis(methyleneoxyethyleneoxy) silicon-phthalocyanine in tumor-bearing mice, J. Photochem. Photobiol. Biol. 50 (1999) 124–128.
[14] G. Roncucci, D. Dei, G. Chiti, L. Fantetti, F. Giuliani, G. Jori, G.M. Rossolini, Antibacterial compositions comprising metal phthalocyanine analogues. patent US 86643282 B2, Monteneli Therapeutics S.R.L., Italy, 2013.
[15] E.D. Baron, C.L. Malbasa, D. Santo-Domingo, P. Fu, J.D. Miller, K.K. Hanneman, N. L. Oleinick, V.C. Colussi, K.D. Cooper, Silicon phthalocyanine (Pc 4) photodynamic therapy is a safe modality for cutaneous neoplasms: results of a phase 1 clinical trial, Laser Surg. Med. 42 (2010) 728–735.
[16] J.D. Miller, E.D. Baron, H. Scull, A. Hsia, J.C. Berlin, T. Mc Cormick, V. Colussi, M.E. Kenney, K.D. Cooper, N.L. Oleinick, Photodyanmic theraphy with the phthalocyanine photosensitizer Pc4: the case experience preclinical mechanistic and early clinical-translational studies, Toxicol. Appl. Pharm. 224 (2007) 290–299.
[17] N.L. Oleinick, A.R. Antunez, M.E. Clay, M.E. Rither, B.D. Kenney, New phthalocyanine photosensitizers for photodynamic therapy, Photochem. Photobiol. 57 (1993) 242–247.
[18] V.R.M. Darwish, S.F. Bloomfield, Effec of ethanol, propylene glycol and glycerol on the interaction of methyl and peopyl *p*-hydroxybenzoate with *Straphylococus aureus* and *Pseudomonas aeruginasa*, Int. J. Pharm. 147 (1997) 51–60.
[19] S. Doron, M. Friedman, M. Falach, E. Sadovnic, H. Zvia, Antibacterial effect of parabens against planktonic and biofilm *Streptococcus sobrinus*, Int. J. Antimicrob. Agents 18 (2001) 575–578.
[20] P.D. Daubre, A. Aljarrah, W.R. Miller, N.G. Coldham, M.J. Sauer, G.S. Pope, Concentrations of parabens in human breast tumours, J. Appl. Toxicol. 24 (2004) 5–13.
[21] Z. Luksiene, A. Zukauskas, Prospects of photosensitization in control of pathogenic and harmful microorganisms, J. Appl. Microbiol. 107 (2009) 1415–1424.
[22] T.C. Pagonic, J. Chen, C.R. Fontana, H. Devalapally, K. Ruggiero, X. Song, F. Foschi, J. Dunham, Z. Skobe, H. Yamazaki, R. Kent, A.C.R. Tanner, M.M. Amiji, N.S. Soukos, Nanoparticle-based endodontic antimicrobial photodynamic therapy, J. Endod. 36 (2) (2010) 322–328.
[23] Y. Ma, R.E. Marquis, Irreversible paraben inhibition of glycolysis by *Streptococcus mutans* GS-5, Lett. App. Microbiol. 23 (1996) 329–333.
[24] T.P. Paulino, K.F. Ribeiro Jr, G. Thedei, A.C. Tedesco, P. Ciancaglini, Use of hand held photopolymerizer to photoinactivate *Streptococcus mutans*, Arch. Oral Biol. 50 (2005) 353–359.
[25] M.E. Kenney, Bromoaluminum phthalocyanine tripyridinate, J. Inorg. Nucl. Chem. 11 (1959) 167.
[26] M.K. Lowery, A.J. Starshak, J.N. Esposito, P.C. Krueger, M.E. Kenney, Dichloro (phthalocyanino) silicon, Inorg. Chem. 4 (1965) 128–132.
[27] B.L. Wheeler, G. Nagasubramanian, A.J. Bard, L.A. Schechtman, D.R. Dininny, M. E. Kenney, A silicon phthalocyanine and a silicon naphthalocyanine: synthesis, electrochemistry, and electrogenerated chemiluminescence, J. Am. Chem. Soc. 106 (1984) 7404–7410.
[28] G.C. Zhang, J.D. Huang, Y.M. Chen, J.C. Sun, H. Liu, N.S. Chen, J.L. Huang, A new silicon phthalocyanine axially substituted by nipagin: synthesis, molecular spectroscopic properties, an in vitro photodynamic activities. Guang Pu, Xue Yu, Guang Pu, Fen Xi. (2005) 25: 10, 1622–1626.
[29] S. Fery-Forgues, D. Lavabre, Are fluorescence quantum yields so tricky to measure? A demonstration using familiar stationery products, J. Chem. Educ. 76 (1999) 1260–1264.
[30] D. Maree, T. Nyokong, K. Suhling, D. Phillips, Effects of axial ligands on the photophysical properties of silicon octaphenoxyphthalocyanine, J. Porphyrins Phthalocyanines 6 (2002) 373–376.
[31] A. Ogunsipe, J.-Y. Chen, T. Nyokong, Photophysical and photochemical studies of zinc(II) phthalocyanine derivatives—effects of substituents and solvents, New J. Chem. 28 (2004) 822–827.
[32] A. Ogunsipe, D. Maree, T. Nyokong, Solvent effects on the photochemical and fluorescence properties of zinc phthalocyanine derivatives, J. Mol. Struct. 650 (2003) 131–140.
[33] Y. Zorlu, F. Dumoulin, M. Durmuş, V. Ahsen, Comparative studies of photophysical and photochemical properties of solketal substituted platinum(II) and zinc(II) phthalocyanine sets, Tetrahedron 66 (2010) 3248–3258.
[34] G.M. Sheldrick, SADABS. Program for Empirical Absorption Correction, Unversity of Gottingen, Germany, 2015.
[35] BrukerAPEX2 (Version 2011.4-1). Bruker AXS Inc. Madison, Wisconsin, USA, 2008.
[36] G.M. Sheldrick, A short history of *SHELX*, Acta Crystallogr. A64 (2008) 112–122.
[37] A.L. Spek, Structure validation in chemical crystallography, Acta Crystallogr. D65 (2009) 148–155.
[38] C.F. Macrae, I.J. Bruno, J.A. Chisholm, P.R. Edgington, P. Mc Cabe, E. Pidcock, L. Rodriguez-Monge, R. Taylor, J.V. Streek, P.A. Wood, Mercury CSD 2. 0 – new features for the visualization and investigation of crystal structures, J. Appl. Crystallogr. 41 (2008) 466–470.
[39] Brandenburg K. DIAMOND 3.1 for Windows. Crystal Impact GbR, Bonn, Germany, 2006.
[40] V. Mantareva, D. Petrova, L. Avramov, I. Angelov, E. Borisova, M. Peeva, D. Wöhrle, Long wavelength absorbing cationic Zn(II)-phthalocyanines as fluorescent contrast agents for B16 pigmented melanoma, J. Porphyrins Phthalocyanines 9 (1) (2005) 47–53.
[41] V. Mantareva, V. Kussovski, I. Angelov, D. Wöhrle, R. Dimitrov, E. Popova, S. Dimitrov, Non-aggregated Ga(III)-phthalocyanines: synthesis and photodynamic effect on pathogenic microorganisms planktonic and biofilms cultures, Photochem. Photobiol. Sci. 10 (1) (2011) 92–102.
[42] X. Leng, D.K.P. Ng, Axial coordination of cobalt(II) porphyrins with bis (pyridinolato) silicon(IV) phthalocyanines, Eur. J. Inorg. Chem. 461 (2007) 4615–4620.
[43] M. Brewis, G.J. Clarkson, M. Helliwell, A.M. Holder, N.B. McKeown, The synthesis and glass-forming properties of phthalocyanine-containing poly (aryl ether) dendrimers, Chem. Eur. J. (2000) 4630–4636.
[44] Z. Zhao, P.-S. Chan, H. Li, K.-L. Wong, R.N.S. Wong, N.-K. Mak, J. Zhang, H.-L. Tam, W.-Y. Wong, D.W.J. Kwong, W.-K. Wong, Highly selective mitochondria-targeting amphiphilic silicon(IV) phthalocyanines with axially ligated Rhodamine B for photodynamic therapy, Inorg. Chem. 51 (2012) 812–821.
[45] J.A. Lacey, D. Phillips, Fluorescence lifetime measurements of disulfonated aluminium phthalocyanine in the presence of microbial cells, Photochem. Photobiol. Sci. 1 (2002) 378–383.
[46] I. Seotsanyana-Mokhosi, N. Kuznetsova, T. Nyokong, Photochemical studies of *tetra*-2,3-pyridinoporphyrazines, J. Photochem. Photobiol. A Chem. 140 (2001) 215–222.
[47] R. Gergova, Tz. Georgieva, I. Angelov, V. Mantareva, S. Valkanov, I. Mitov, Dimitrov Sl Photodynamic therapy with water-soluble phtalocyanines against bacterial biofilms in teeth root canals, Progress in Biomedical Optics and Imaging – Proc SPIE, Int. Soc. Opt. Eng. 8427 (842744) (2012) 1–12.
[48] V. Mantareva, I. Angelov, V. Kussovski, D. Wöhrle, S. Dimitrov, Metallophthalocyanines as photodynamic sensitizers for treatment of pathogenic bacteria. Uptake and photoinactivation properties, Comp. Rend. Bulg. Acad. Sci. 1 (2010) 77–84.
[49] V. Mantareva, I. Angelov, V. Kussovski, R. Dimitrov, L. Lapok, D. Wöhrle, Photodynamic efficiency of water-soluble Si(IV) and Ge(IV) phthalocyanines towards *Candida albicans* planktonic and biofilm cultures, Eur. J. Med. Chem. 46 (2011) 4430–4440.
[50] T.N. Demidova, M.R. Hamblin, Effect of cell-photosensitizer binding and cell density on microbial photoinactivation, Antimicrob. Agents Chem. 49 (2005) 2329–2335.
[51] G. Bertoloni, F. Rossi, G. Valduga, G. Jori, J.E. Van Lier, Photosensitizing activity of water- and lipid-soluble phthalocyanines on *Escherichia coli*, FEMS Microbiol. Lett. 7 (1990) 149–156.